Materials Science in Semiconductor Processing 13 (2010) 34–40

Contents lists available at ScienceDirect

Materials Science in Semiconductor Processing

journal homepage: www.elsevier.com/locate/mssp

The effects of surface states and series resistance on the performance of Au/SnO_2/n-Si and Al/SnO_2/p-Si (MIS) Schottky barrier diodes

D.E. Yıldız [a,*], Ş. Altındal [b], Z. Tekeli [b], M. Özer [b]

[a] Physics Department, Faculty of Arts and Sciences, Hitit University, 19030, Çorum, Turkey
[b] Physics Department, Faculty of Arts and Sciences, Gazi University, 06500, Ankara, Turkey

ARTICLE INFO

Available online 18 April 2010

Keywords:
Au/SnO2/n-Si and Al/SnO2/p-Si SBDs
Surface states
Series resistance
Insulator layer
I–V–T characteristics

ABSTRACT

We have fabricated two types of Schottky barrier(SBDs),Au/SnO_2/n-Si (MIS1) and Al/SnO_2/p-Si (MIS2), to investigate the surface (N_{ss}) and series resistance (R_s) effect on main electrical parameters such as zero-bias barrier height (Φ_{Bo}) and ideality factor (n) for these SBDs. The forward and reverse bias current–voltage (I–V) characteristics of them were measured at 200 and 295 K, and experimental results were compared with each other. At temperatures of 200 and 295 K, Φ_{Bo}, n, N_{ss} and R_s for MIS1 Schottky diodes (SDs) ranged from 0.393 to 0.585 eV, 5.70 to 4.75, 5.42×10^{13} to 4.27×10^{13} $eV^{-1}cm^{-2}$ and 514 to 388 Ω, respectively, whereas for MIS2 they ranged from 0.377 to 0.556 eV, 3.58 to 2.1, 1.25×10^{14} to 3.30×10^{14} $eV^{-1}cm^{-2}$ and 312 to 290 Ω, respectively. The values of n for two types of SBDs are rather than unity and this behavior has been attributed to the particular distribution of N_{ss} and interfacial insulator layer at the metal/semiconductor interface. In addition, the temperature dependence energy density distribution profiles of N_{ss} for both MIS1 and MIS2 SBDs were obtained from the forward bias I–V characteristics by taking into account the bias dependence of effective barrier height (Φ_e) and R_s. Experimental results show that both N_{ss} and R_s values should be taken into account in the forward bias I–V characteristics. It has been concluded that the p-type SBD (MIS2) shows a lower barrier height (BH), lower R_s, n and N_{ss} compared to n-type SBD (MIS1), which results in higher current at both 200 and 295 K.

1. Introduction

The surface stability and the formation of an insulator layer between metal and semiconductor play a very important role in the fabrication of MIS type SBDs. These types of devices have gained increasing importance due to a wide variety of optoelectronic and high frequency applications in the electronic industry and their electrical characteristics have been extensively studied till now [1–13]. But the formation mechanisms of interfacial insulator layer and barrier height at the M/S interface, conduction mechanisms, the effect of series resistance and surface states on I–V characteristics have not been completely clarified. Pure thermionic theory (n=1) is true when we neglect the role of Rs and insulator layer. For instance, the existence of an insulator layer at the M/S interface, native or deposited, the SBD transforms into a MIS type SBD and its I–V characteristics will consequently deviate considerably from those expected in an ideal case. The presence of an insulating layer may cause a surface state charge with bias due to an additional field in the interfacial layer, effecting the diode electrical characteristics [4–7,14–23]. Recently, the formation of an insulator layer on Si crystal, such as SnO_2 [23], Si_3N_4 [10], and TiO_2 [22] films, has been investigated as a potential material to replace SiO_2.

Another effect on the main SBDs parameters is the series resistance associated with the semiconductor bulk,

* Corresponding author. Tel.: +90 312 211 2397; fax: +90 388 311 2639.
E-mail address: dilberesra@hotmail.com (D.E. Yıldız).

1369-8001/$ - see front matter © 2010 Elsevier Ltd. All rights reserved.
doi:10.1016/j.mssp.2010.02.004

which causes the voltage drop across the junction to be less than the applied voltage between the terminals of the diode. In the case of a diode with a high series resistance, the *I–V* characteristics of the Schottky diode is different from the expected one, especially in the high forward bias region [2,4–6,17–20]. Cheung's plots are obtained from data of the downward concave curvature region in the forward bias semi-logarithmic *I–V* plot, which results from the series resistance and the effects on interfacial parameters [18]. In general, the N_{ss} can be subdivided into two groups. One of these groups communicates most rapidly with the metal and the other group with the semiconductor. On the other hand, one of these groups is in equilibrium with metal and the other group is in equilibrium with the semiconductor. These two groups are dependent on the thickness of interfacial insulator layer and the communication with the semiconductor, increasing with increase in insulator layer thickness [3]. Card and Rhoderick [3], Horvath [21] and Tseng and Wu [16] estimated the surface state density located at the insulator layer/silicon interface and examined the effects of the interface states on the ideality factor of the forward bias *I–V* characteristics. In the past, the Gaussian distribution of BHs has been widely accepted to correlate with experimental data [6,10,11,19]. In some studies, the effects of native oxide layer [9] and thermal-growth oxide layer [24] on some electronic parameter of Schottky diodes have been studied. Yıldız et al. [14] explained the importance of the fact that the neutral-region resistance value should be considered in calculating the surface state density distribution from the non-ideal forward bias *I–V* characteristic.

The main purpose of this study is to present the results of a systematic investigation of the role of R_s and N_{ss} on the forward bias *I–V* characteristics of Au/SnO_2/n-Si (MIS1) and Al/SnO_2/p- Si (MIS2) SBDs at low (200 K) and room (295 K) temperatures, and the obtained experimental results were compared with each other. Therefore, the temperature dependence energy density distribution profiles of N_{ss} for both the MIS1 and MIS2 were obtained from forward bias *I–V* measurements by taking into account the bias dependence of effective barrier height (Φ_e), ideality factor (n) and series resistance (R_s).

2. Experimental procedure

The Au/SnO_2/n-Si (MIS1) and Al/SnO_2/p-Si (MIS2) Schottky barrier diodes (SBDs) were fabricated on Si wafers having, respectively, (1 1 1) and (1 0 0) orientations, 350 and 280 μm thicknesses, and ≈4, 2 Ω cm resistivities. The Si wafers were degreased for 5 min in boiling trichloroethylene, acetone and ethanol consecutively and then etched in, first, H_2SO_4, H_2O_2 and 20% HF solution, then $6HNO_3$:1HF:$35H_2O$ and 20% HF solution. Preceding each cleaning step, the wafers were rinsed thoroughly in de-ionized water of 18 MΩ cm. For the fabricating of SnO_2/n-Si (MIS1) and Al/SnO_2/p-Si (MIS2) SBDs, immediately after surface cleaning, the high purity gold (Au) and aluminum (Al) metal (99.999%), respectively, with a thickness of 2500 Å were thermally evaporated from tungsten filament onto the whole back surface of the Si wafers at a pressure of $\approx 1\times10^{-6}$ Torr in liquid nitrogen trapped oil-free ultrahigh vacuum pump system. To obtain a low-resistivitiy ohmic back contact, both evaporated Au and Al back contact Si wafers were sintered in vacuum at about 400 °C and 4 min in N_2 atmosphere. Immediately after ohmic back contact, for two type of Si wafers, a thin layer of SnO_2 was grown on the Si substrate by spraying a solution consisting of 32.21 wt% of ethyl alcohol (C_2H_5OH), 40.35 wt% of de-ionised water (H_2O) and 27.44 wt% of stannic chloride ($SnCl_4\cdot5H_2O$) on the substrate, which was maintained at a constant temperature of 400 °C. The temperature of the substrates was monitored by chromel–alumel thermocouple fixed on the top surface of the Si substrate. The variation in the substrate temperature during spray was maintained within ±2 °C with the help of a temperature controller. The rate of spraying was kept at about 30 cc/min by controlling the carrier gas flow meter. N_2 was used as the carrier gas. SnO_2 dots were 4 mm in diameter. After spraying process, the rectifying contacts in the form of circular dots of 2 mm in diameter and 2500 Å thick Au and Al, were deposited onto the SnO_2 surface of the wafer in a similar manner as the back contacts. Metal layer thickness and deposition rates were monitored with the help of a digital quartz crystal thickness monitor. The deposition rates were about 1–3 Å/s. The interfacial insulator layer thicknesses, δ, for Au/SnO_2/n-Si (MIS1) and Al/SnO_2/p-Si (MIS2) Schottky barrier diodes were obtained from high frequency (1 MHz) using the equation for insulator capacitance ($C_{ox}=\varepsilon_i\varepsilon_o A/d$) as 32 and 28 Å, respectively, where $\varepsilon_i=7\varepsilon_o$ [1,9] and ε_o is the permittivity of free space.

The forward bias *I–V* measurements of Au/SnO_2/n-Si (MIS1) and Al/SnO_2/p-Si (MIS2) SBDs were carried out using a Keithley 220 current source and a Keithley 614 electrometer. The measurements were performed at 200 and 295 K using a temperature controlled Janis vpf-475 cryostat. The sample temperature was always monitored by means of a copper-constantan thermocouple and a Lakeshore 321 auto-tuning temperature controller with sensitivity better than ±0.1 K. All measurements were carried out with the help of a microcomputer through an IEEE-488 ac/dc converter card.

3. Results and discussion

For a MIS type SBDs with a Rs, it is considered, according to the thermionic emission (TE) mechanism corrected by tunneling, that the relation between the applied forward bias voltage V ($V>3$ kT/q) and the current is expressed as [1,2,18,24,25]

$$I = I_o\exp\left(\frac{q}{nkT}(V-IR_s)\right)[1-\exp(-q(V-IR_s)/kT)] \quad (1a)$$

where I_o is the reverse saturation current derived from the straight line intercept of the current zero bias and is given by

$$I_o = A^*AT^2\exp(-q\Phi_{Bo}/kT) \quad (1b)$$

where the quantities A^*, A, and Φ_{Bo} are the effective Richardson constants for n- and p-Si and are equal to 120

and 32 A/cm^2 K^2, respectively, the rectifier contact area and the zero-bias barrier height, respectively. Ideality factor is a measure of conformity at the diode to pure thermionic emission and is contained in the slope of straight line region of the forward bias logarithmic characteristics of I–V through the relation

$$n = \frac{q}{kT}\left[\frac{d(V)}{d\,\mathrm{Ln}(I)}\right] \tag{2}$$

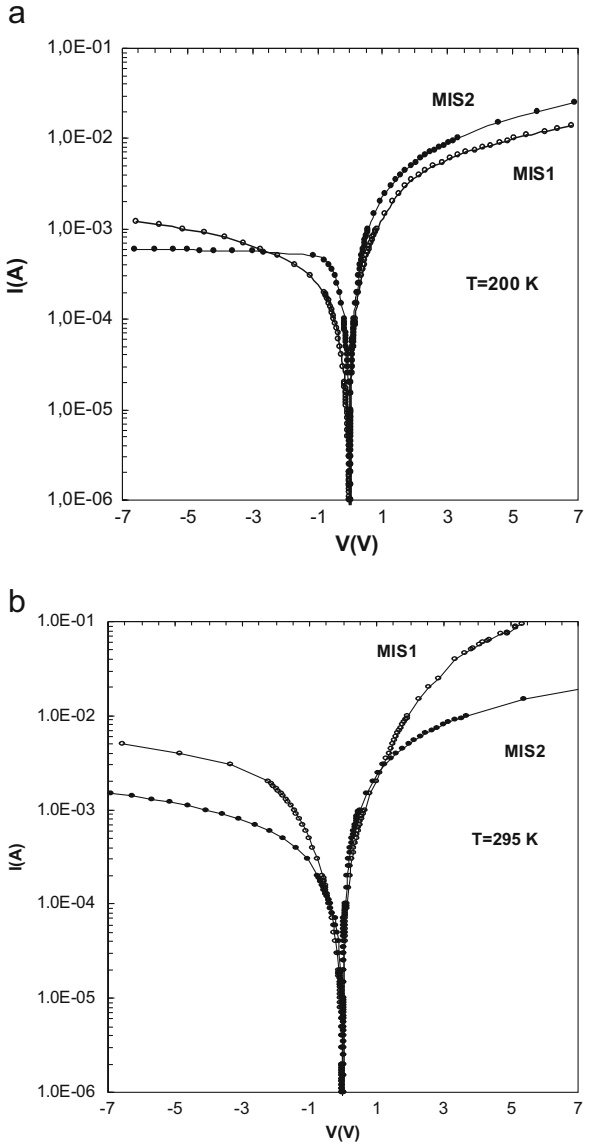

Fig. 1. The experimental forward and reverse bias Ln I–V characteristics of MIS1 and MIS2 SBDs at 200 and 295 K, respectively.

Fig. 1 shows the experimental forward and reverse bias Ln I–V characteristics of the sample MIS1 and MIS2 at the temperatures 200 and 295 K, respectively.

The Φ_{Bo} and n values of these samples were calculated with the help of Eqs. (1b) and (2) from the current-axis intercept and slope of the linear region of the Ln I–V plots, respectively. At the temperatures of 295 and 200 K, the values of n are 4.75 and 5.7 for the sample MIS1, and 2.1 and 3.58 for the sample MIS2, respectively. The values of Φ_{Bo} for the MIS1 and MIS2 were found to be 0.585 and 0.556 eV (at 295 K), and 0.393 and 0.377 eV (at 200 K), respectively. The Φ_{Bo} and n values of MIS1 and MIS2 obtained from forward bias I–V for two different temperatures are given in Table 1. As can be shown in Table 1, a decrease in barrier heights and an increase in ideality factors with decrease in temperature for both diodes are at first sight indicative of deviation from the pure TE-mechanism. The possible reason could be explained on the basis of a TE-mechanism with Gaussian distribution [26]. In addition, the tunneling parameter, E_{oo}, that determines the relative importance of tunneling in thermionic-field emission (TFE) or field emission (FE) and thermionic emission-diffusion (TED) is given by [1]. The FE becomes important when $E_{oo} \gg kT/q$, whereas the TFE dominates when $E_{oo} \approx kT/q$, and thermionic emission-diffusion if $E_{oo} \ll kT/q$. In the present case, N_D is 5.24×10^{21} m^{-3} at 200 K and 1.37×10^{22} m^{-3} at 295 K for MIS1. The corresponding E_{oo} value turns out to be 0.20 meV at 200 K and 0.63 meV at 295 K. Here, the value of $E_{oo} \ll kT/q$. Therefore, the possibility of the FE and TFE can easily be ruled out. The same calculations for E_{oo} were made for the sample MIS2 and similar results were obtained.

The series resistance is important in the downward concave curvature of the forward bias I–V characteristics, while the other two parameters are important in both linear and non-linear regions of I–V characteristics. Therefore the ideality factor and the series resistance were evaluated using a method developed by Cheung and Cheung [18] in the high current range where the I–V characteristic is not linear. According to this method from Eq. (1a), the following functions can be written as

$$\frac{dV}{d\,\mathrm{Ln}\,I} = n\frac{kT}{q} + R_s I \tag{3}$$

Table 1
The experimental values of some electrical parameters obtained from the forward bias I–V characteristics at two different temperatures for MIS1 and MIS.

T (K)	Sample	n (I–V)	n ($dV/d\mathrm{Ln}\,I$)	Φ_{Bo} (I–V) (eV)	N_{ss} (eV^{-1} cm^{-2})	$R_s(dV/d\mathrm{Ln}\,I)$ (Ω)	$R_s(H(I))$ (Ω)
295	**MIS1**	4.75	4.72	0.585	4.27×10^{13}	388	392
	MIS2	2.10	1.97	0.556	1.25×10^{14}	290	276
200	**MIS1**	5.70	5.77	0.393	5.42×10^{13}	514	519
	MIS2	3.58	3.54	0.377	3.30×10^{14}	312	323

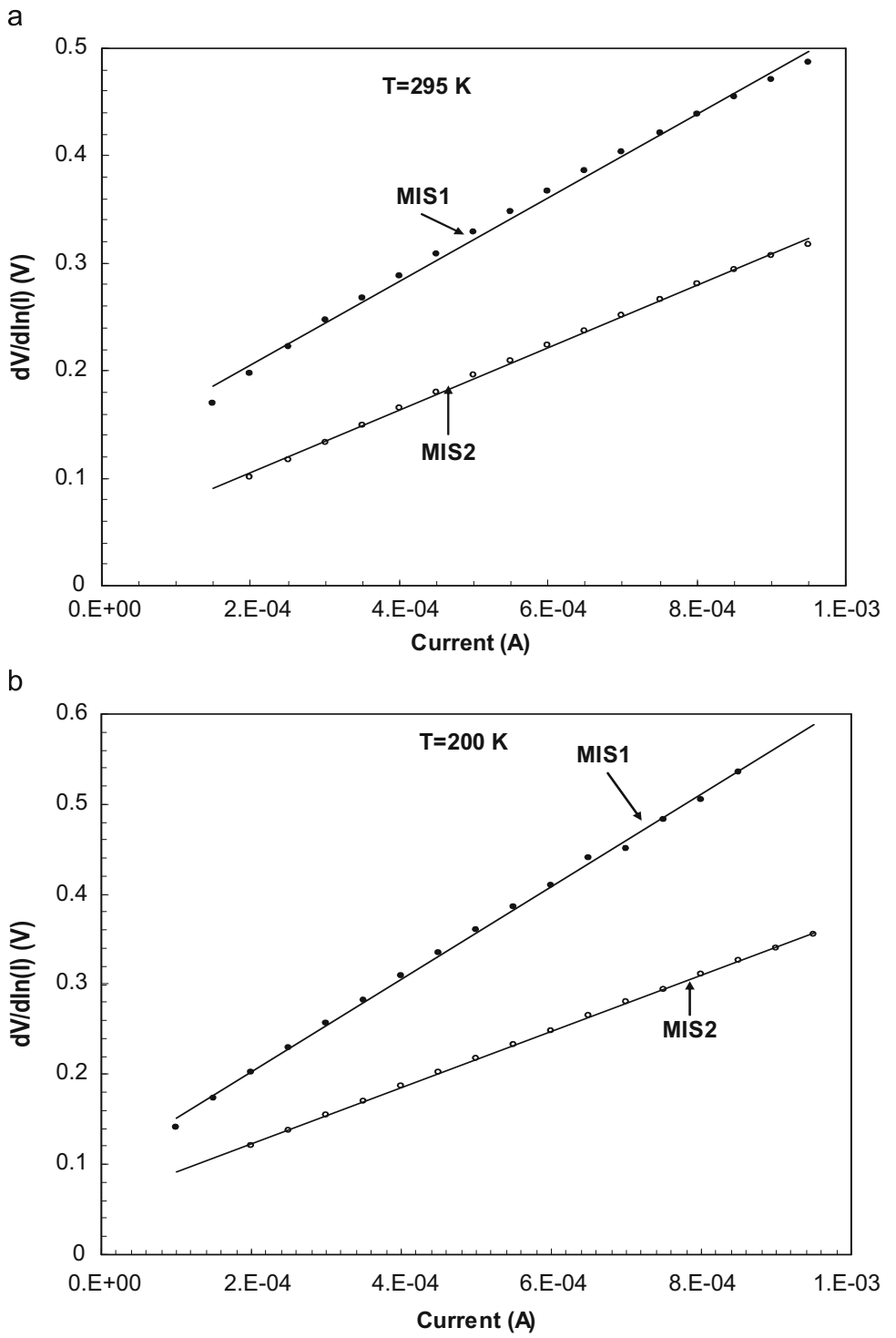

Fig. 2. The $dV/d\,\mathrm{Ln}(I)$ vs I plots for MIS1 and MIS2 SBDs at 200 and 295 K, respectively.

$$H(I) = V - n\frac{kT}{q}\,\mathrm{Ln}\left(\frac{1}{AA^{*}T^{2}}\right) = n\Phi_{B} + R_{s}I \tag{4}$$

and $H(I)$ is given as follows:

$$H(I) = n\Phi_{B} + R_{s}I \tag{5}$$

Figs. 2 and 3 show experimental $dV/d(\mathrm{Ln}\,I)$ vs I and $H(I)$ vs I plots, respectively, at two different temperatures for Au/SnO_2/n-Si (MIS1) and Al/SnO_2/p-Si (MIS2) SBDs. Eq. (3) should give a straight line for the data of downward curvature region in the forward bias I–V characteristic.

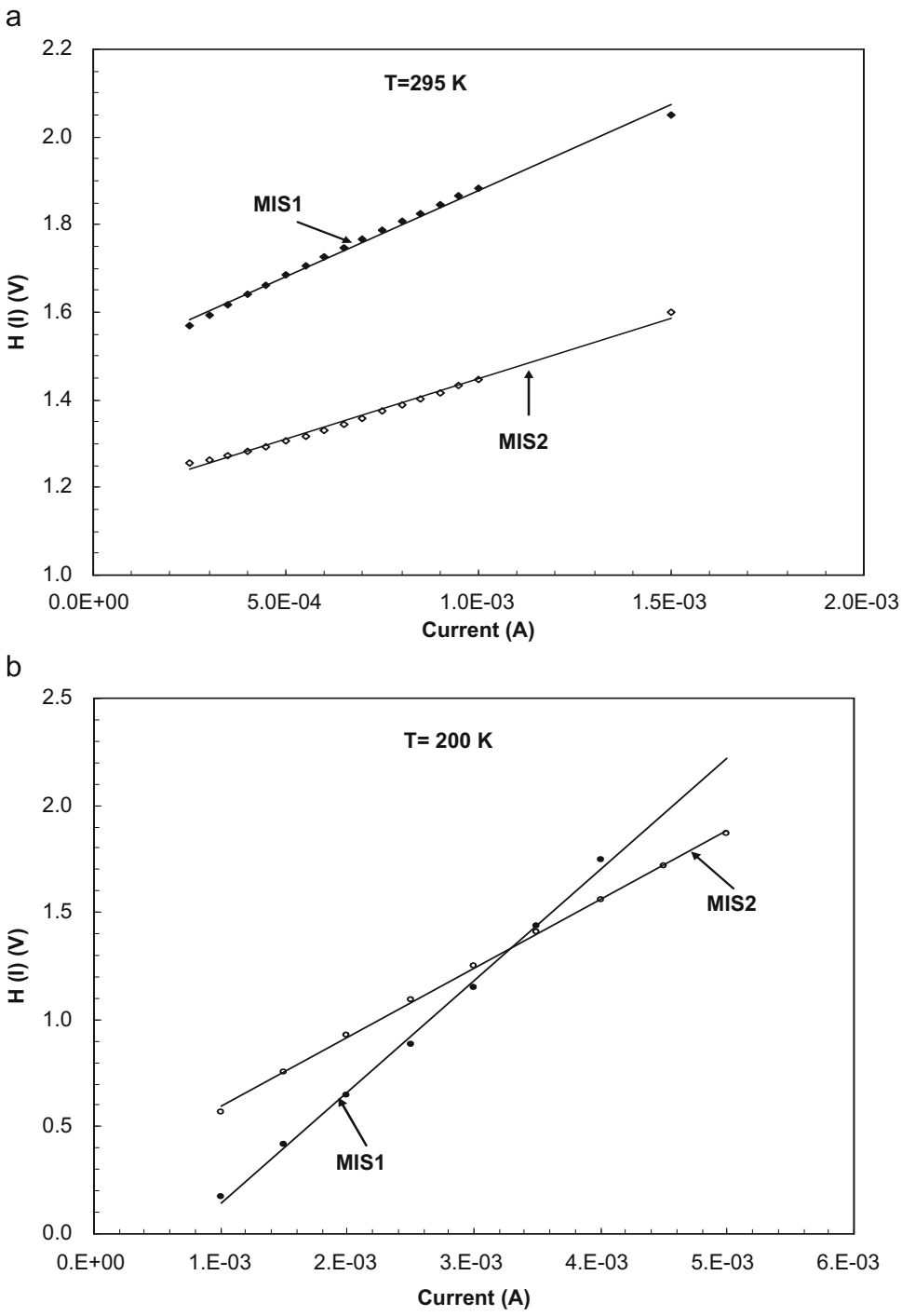

Fig. 3. The $H(I)$ vs I plots of MIS1 and MIS2 SBDs at 200 and 295 K, respectively.

Thus, a plot of $dV/d(\mathrm{Ln}\, I)$ vs I (Fig. 2) will give R_s as the slope and nkT/q as the current–axis intercept. Using the n value determined from Eq. (3) and the data of downward curvature region, a plot of $H(I)$ vs I(Fig. 3) according to Eq. (5) will also give a straight line with current–axis. The values of R_s and n of the MIS1 and MIS2 diodes obtained from Figs. 1–3 are given in Table 1. As can be seen in Table 1, as the linear range of the forward I–V plots is reduced, the values of n calculated from thermionic emission (TE) theory are poorer than those calculated from Cheung's functions. Also, the obtained R_s values by two different Cheung functions are in good agreement with each other. For the p-type SBD (MIS2) shows a lower barrier height (BH), lower R_s, n and N_{ss} according to n-type

SBD (MIS1), which result in higher current of both 200 and 295 K.

For two types of SBDs, the values of n are greater than unity and R_s is sufficiently large at each temperature. This behavior of n and R_s can be attributed to the presence of an oxide layer (SnO_2) between the metal and the semiconductor. For a sufficiently thick interface insulator layer, the interface states are in equilibrium with the semiconductor, and they cannot interact with the metal [1–4,14]. In the downward curvature region of forward bias *I–V* plots of the samples MIS1 and MIS2 at sufficiently large voltages, the ideality factor *n* is rather controlled by the interface states and series resistance. The effect of R_s is usually modeled with a series combination of a diode and a resistor with resistance R_s, through which the current flows. When a forward bias *V* is applied across the MIS type SBD, the applied bias voltage *V* will be shared by the interfacial layer (V_i), the depletion layer (V_s) and the series resistance combination of the device R_s, and thus *V* can be written as

$$V = V_s + V_i + IR_s \tag{6}$$

when the interfacial layer is sufficiently thick and the transmission probability between the metal and the interface states is very small, the effective barrier height Φ_e is assumed to be bias-dependent due to the presence of an interfacial insulator layer and interface states located between the interfacial layer and the semiconductor interface, and is given by [4,6,8]

$$\Phi_e = \Phi_{Bo} + \beta(V - IR_s) = \Phi_{Bo} + \left(1 - \frac{1}{n(V)}\right)(V - IR_s) \tag{7}$$

by considering the applied voltage dependence of the barrier height, where β is the voltage coefficient of the effective barrier height (Φ_e) used in place of the barrier height Φ_{Bo} and it is a parameter that combines the effect of both the values of N_{ss} and interfacial layer thickness for cases in which the N_{ss} are in equilibrium with the semiconductor [25,26]. For an MIS diode the ideality factor *n* becomes greater than unity as proposed by Card and Rhoderick [3]

$$n(V) = 1 + \frac{\delta}{\varepsilon_i}\left[\frac{\varepsilon_s}{W_D} + qN_{ss}(V)\right] \tag{8a}$$

where ε_s and ε_i are the permittivity of the semiconductor and the interfacial layer, respectively, δ is the thickness of insulator layer, and W_D is the width of the

The values of N_{ss} were obtained from equation (8b) by substituting the values of insulator layer thickness (d), the values of voltage dependent ideality factors (n (V)) and space charge width (W_D). This expression is identical to Eq. (18) of Card and Rhoderick [3], and is reduced to

$$N_{ss}(V) = \frac{1}{q}\left[\frac{\varepsilon_i}{\delta}(n(V) - 1) - \frac{\varepsilon_s}{W_D}\right] \tag{8b}$$

ε_i=7 ε_o, ε_s=11.8ε_o in Eq. (8b), the N_{ss} distributions for samples MIS1 and MIS2 were calculated by taking into account the contribution of the series resistance. In a p-type semiconductor (MIS2), the energy of N_{ss} with respect to the top of the valence band E_v at the surface of the

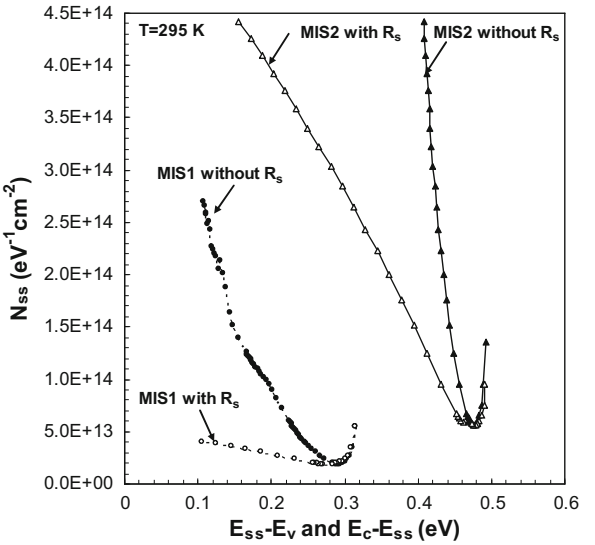

Fig. 4. The density distribution profiles of N_{ss} curves as a function of energy deduced from the forward bias *I–V* data at 295 K for MIS1 and MIS2 SBDs.

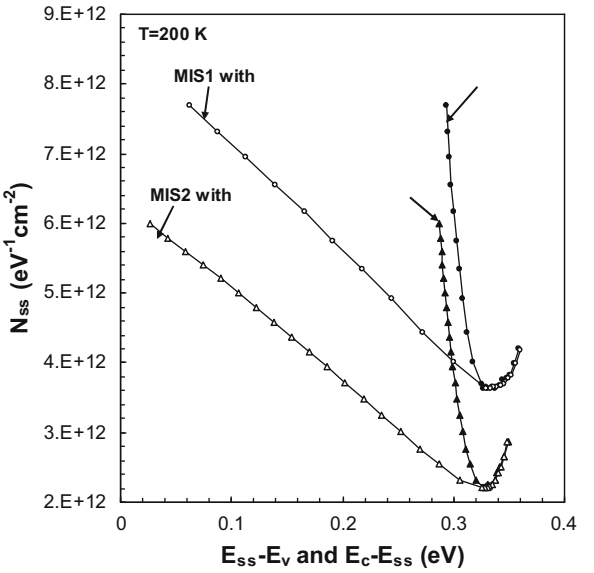

Fig. 5. The density distribution profiles of N_{ss} curves as a function of energy deduced from the forward bias *I–V* data at 200 K for MIS1 and MIS2 SBDs.

semiconductor is given by

$$E_{ss} - E_v = q(\Phi_e - V) \tag{9a}$$

Similarly, in an n-type semiconductor (MIS1), the energy of N_{ss} with respect to the bottom of conductance band E_c at the surface of the semiconductor is given by

$$E_c - E_{ss} = q(\Phi_e - V) \tag{9b}$$

where *V* is the forward applied bias voltage drop across the depletion layer and Φ_e is the effective barrier height. The density distribution profiles of N_{ss} as a function of

energy are deduced from the forward bias *I–V* data for MIS1 and MIS2 at two different temperatures (295 and 200 K) and are given in Figs. 4 and 5, respectively.

Fig. 4 shows the energy distribution profile of the N_{ss} with and without taking into account R_s obtained from the forward bias *I–V* characteristics of the fabricated samples at room temperature. As can be seen in Figs. 4 and 5, the values of N_{ss} obtained taking into account the series resistance values are lower than those obtained without considering the series resistance. Furthermore, in the calculation made without considering the series resistance value of the devices, the N_{ss} value of sample MIS2 is lower than that of sample MIS1 in the same energy position. Similar results have been reported by Türüt et al. [27] and Singh [28]. Also, when the series resistance value is taken into account, the N_{ss} value of sample MIS2 is also larger than that of sample MIS1 in the same energy position. At the same time, the value of N_{ss} in diode with R_s is almost one order of magnitude larger than the diode without R_s [27–29].

From the above explanation and Figs. 4 and 5, the concavity of the forward bias *I–V* curves in the higher voltage region increases with increase in series resistance value. The above explanations clearly show that the series resistance value should be taken into account in determining the interface state density distribution profile and other main diode parameters such as barrier height and ideality factor.

4. Conclusion

In order to investigate the effects of N_{ss} and R_s on the main electrical parameters, we have fabricated two types of Au/SnO_2/n-Si (MIS1) and Al/SnO_2/p-Si (MIS2) SBDs. The *I–V* reverse bias current–voltage (*I–V*) characteristics of them were measured at 200 and 295 K. The forward bias *I–V* characteristics show the downward concave curvature region in the sufficiently high forward bias due to the effect of R_s. Experimental results show that the p-type SBD (MIS2) has a lower barrier height (BH), R_s, n and N_{ss} compared to n-type SBD (MIS1). The high values of ideality factor for two types of diodes at each temperature were attributed to the presence of the insulator layer at the M/S interface and the particular distribution of N_{ss} at the semiconductor/insulator interface. In addition, the energy density distribution profiles of N_{ss} for both MIS1 and MIS2 SBDs were obtained from the forward bias *I–V* characteristics by taking into account the bias dependence of effective barrier height (Φ_e) and R_s. The values of N_{ss} rise from midgap towards the top of valence band as a U-shape distribution for each diode. The obtained value of N_{ss} without taking into account the R_s of the devices is almost one order of magnitude larger than the N_{ss} values obtained by taking into account the R_s. Therefore, to obtain an accurate density distribution of N_{ss} from the forward bias *I–V* characteristics, the series resistance value should be taken into consideration apart from the ideality factor.

References

[1] Sze SM. Physics of Semiconductor Devices, 2nd Edn. New York: Willey; 1981 p. 850.
[2] Rhoderick EH, Williams RH. Metal-Semiconductor Contacts, 2nd Ed. Oxford: Clarendon Press; 1988.
[3] Card. HC, Rhoderick EH. J. Phys. D: Appl. Phys. 1971;4:1589.
[4] Cova P, Singh A, Medina A, Masut RA. Solid-State Electron. 1998;42:477.
[5] Cowley AM, Sze SM. J. Appl. Phys. 1965;36:3212.
[6] Altındal Ş, Dökme İ, Bülbül MM, Yalçın N, Serin T. Microelectron. Eng. 2006;83(3):499.
[7] Aboelfotoh MO, Cros A, Svensson BG, Tu KN. Phys. Rev. B 1990;41:9819.
[8] Singh A, Reinhardt KC, Anderson WA. J. Appl. Phys. 1990;68(7):3475.
[9] Altındal Ş, Kanbur H, Tataroğlu A, Bülbül MM. Physica B 2007;399:146.
[10] Zeyrek S, Altındal Ş, Yüzer H, Bülbül MM. Appl. Surf. Sci. 2006;252(8):2999.
[11] Hudait MK, Krupanidhi SB. Mater. Sci. Eng. B 2001;87:141.
[12] Chattopadhyay P, Daw AN. Solid-State Electron. 1986;29:555.
[13] Karataş Ş, Altındal Ş, Türüt A, Özmen A. Appl. Surf. Sci. 2003;217:250.
[14] Yıldız DE, Altındal Ş, Kanbur H. J. Appl. Phys. 2008;103:124502.
[15] Hanselaer PL, Laflere WH, Van Meirhaeghe RL, Cardon F. J. Appl. Phys. 1984;56:2309.
[16] Tseng HH, Wu CY. Solid State Electron. 1987;30:383.
[17] Norde H. J. Appl. Phys. 1979;50(7):5052.
[18] Cheung SK, Cheung NW. Appl. Phys. Lett. 1986;49:85.
[19] Chand S. Semicond. Sci. Technol. 2004;19:82.
[20] Dökme İ, Altındal Ş. Semicond. Sci. Technol. 2006;21:1053.
[21] Horvath ZS. J. Appl. Phys. 1988;63(3):976.
[22] Pakma O, Serin N, Serin T, Altındal Ş. J. Appl. Phys. 2008;104:014501.
[23] Ozer M, Yıldız DE, Altindal Ş, Bülbül MM. Solid State Electron. 2007;51(6):94.
[24] Dökme İ. Physica B. In Press; 2006.
[25] Chand S, Kumar J. J. Appl. Phys. 1996;80:288.
[26] Werner JH, Güttler HH. J. Appl. Phys. 1993;73:1315.
[27] Türüt A, Bati B, Kökçe A, Sağlam M, Yalçın N. Phys. Scr. 1996;53:118.
[28] Singh A. J. Appl. Phys. 1990;68(7):3475.
[29] Tataroğlu A, Altındal Ş. Nucl. Instrum. Method A 2007;580: 1588.